Journal of Physics: Conference Series

PAPER • OPEN ACCESS

CFD study of a CI engine powered in the dual-fuel mode with syngas and waste vegetable oil

To cite this article: M Costa *et al* 2021 *J. Phys.: Conf. Ser.* **1868** 012014

CFD study of a CI engine powered in the dual-fuel mode with syngas and waste vegetable oil

M Costa[1], M V Prati[1], L De Simio[1], S Iannaccone[1] and D Piazzullo[1]

[1]Istituto Motori, CNR, Viale Marconi, 4 – 80125 Naples, Italy
m.costa@im.cnr.it

Abstract. Syngas production from biomass gasification and its use in combined heat and power (CHP) generation systems is a feasible alternative to traditional fuels in Internal Combustion Engines (ICEs), although its quality is poorer in terms of calorific value and energy density. Therefore, a viable option for its exploitation can be assured if ICEs operate in dual-fuel (DF) mode, where employing non-edible oils (as Waste Vegetable Oils, WVO) as a further residual material may solve issues related both to the utilization of diesel fuels and to the high costs for biodiesel production. The practice promotes a virtuous circle to enhance material recovery without disposal. A combined experimental-numerical activity for the analysis of the performances of a Compression Ignition (CI) engine in the DF mode with syngas and WVO is here presented. An appropriate pre-heating system is mounted on the engine injection line to reduce the WVO viscosity. Experimental data collected in terms of in-cylinder pressure cycle, heat release rates and main pollutants at different loads are used to validate a properly developed three-dimensional (3D) Computational Fluid Dynamics (CFD) model, that helps investigating the detail of the syngas fuelling on power output and emissions.

1. Introduction

Compression Ignition (CI) engines are largely employed for power generation and heavy-duty automotive applications, due to their higher efficiency with respect to Spark Ignition (SI) engines. However, the carbon dioxide emissions (CO_2) from fossil fuels led to the need for alternatives characterised by a renewable nature, especially for steady applications [1]. One of the most promising solutions is syngas from biomass gasification, a gaseous mixture composed by carbon monoxide (CO), CO_2, hydrogen (H_2), methane (CH_4), nitrogen (N_2) and other minor hydrocarbons. Small-to-micro scale power plants generally exploit the primary power of this gaseous source in ICEs for the combined production of electrical and thermal power. However, its quality is significantly poorer than diesel oil, with a Lower Heating Value (LHV) ranging from 4-6 MJ/Nm^3 and an energy density of about 2,4 MJ/Nm^3, leading to an estimated 30% derating under this fuelling condition [2]. Syngas autoignition temperature is higher than the one achieved at the end of the compression phase, thus DF operation modes reveal fundamental for syngas combustion in CI engines, where the mixture is ignited by a pilot injection of liquid fuel in the combustion chamber [3].

High number of experiments have been conducted to explore the potentiality of dual-fuel operations in CI engines, where the effects of different syngas compositions [4] and engine loads [5] have been assessed. In addition, massive researches have been also performed through CFD methods to optimize the two fuels dosage and the reacting flow-field [3]. However, most works dealt with the implementation of diesel or biodiesel fuels to ignite the mixture, while to the best of authors knowledge, only few dealt with the experimental analysis of waste vegetable oil [6]. Indeed, the suitability of this renewable source when directly employed in CI engines has been proved without any modification to the engine architecture or the injection system and as only requiring low mechanical treatments to the fuel to reduce its high viscosity deriving from fractions of fatty acids from cooking processes [7]. Moreover, the implementation of these non-edible oils solves issues related both to the exploitation of diesel fuels and to the high costs for biodiesel production, promoting a virtuous circle to enhance material recovery without disposal.

In the present work, a combined experimental-numerical activity for the analysis of the performances of a CI engine fuelled in the DF mode with syngas and WVO is presented. An appropriate pre-heating system is mounted on the injection line to reduce WVO viscosity, while the engine performances are experimentally characterised at different loads. The data collected in terms of in-cylinder pressure cycle, heat release rates and main pollutants at the exhaust are used to validate a properly developed three-dimensional (3D) Computational Fluid Dynamics (CFD) model that is then used to investigate the effect of the syngas fuelling on power output and emissions and that reveals as a reliable tool to be used to optimise the relative amount of the two different fuels.

2. Experimental Layout

The experimental tests are carried out at 1500 rpm under different load conditions on a 4-cylinder, 1.9 litre displacement, diesel engine with a compression ratio of 18:1. The engine is powered under both single fuel (Diesel and WVO) and under DF conditions (with liquid WVO and a ternary syngas). This last is a mixture of CH_4 and H_2 (40%-60% by volume) injected near the intake valves, with addition of N_2 upstream of the compressor, whose proportion is chosen to simulate the chemical characteristics of a reference syngas, obtained from gasification of sewage sludge. The energy content of the gaseous mixture together with that of the pilot injection provides the same power as for an operation with only WVO. As for the two liquid fuels tested, two separate lines were used up to the engine, with two separate tanks and consumption measurement systems to avoid mutual contamination, providing for a sort of washing phase of the engine fuel line system (pump, ducts and injectors), with the discharge of the mixed fuel in a third tank, in the transition from one supply to another. The temperature of the WVO was maintained at about 75 ± 5°C, to reduce viscosity, hence to melt the fat from the heavier fractions present in the vegetable fuel. This was accomplished by heating the 50-litre tank with two 500 W electric bands controlled by thermostats.

The engine intake air was measured by a viscous meter. The CH_4/H_2 mixture consumption was evaluated through a Micromotion Elite Coriolis mass flow meter; the N_2 mass flow rate through a BROOKS thermal mass flow meter. Diesel consumption was measured with an AVL gravimetric system. WVO consumption was obtained by weighing the tank, with the relative acquisition times, necessary for a significant reduction during engine operation. The measurement of the exhaust gaseous emissions was made by using a Beckmann 404 with flame ionization detector for total hydrocarbons (THC), ABB Limas11 with ultraviolet radiation detector for NOx, ABB Uras 14 with non-dispersive infra-red detector for CO, CO_2 and with electrochemical sensor for O_2. For the acquisition of the in-cylinder pressure cycle, a quartz piezoelectric transducer (Kistler 6058A) was used together with a Kistler signal amplifier (Charge Amplifier, Type 5064), an AVL angular marker, set with a resolution 0.5 CAD, and an AVL IndiCom module.

2.1 Engine behavior

A first comparison was made between the engine fuelled by commercial diesel and WVO. Results shown in table 1 are an average of four measurements and refer to the same fuel injection times, since the injection pressure was used to change the fuel mass flow rate. An increase in fuel mass consumption in the case of WVO was registered to achieve the same load, mainly due to the different calorific value of the two fuels: almost 42 MJ/kg for diesel and 37 MJ/kg for WVO. Moreover, there was a need for a slight increase in the injection pressure per unit of fuel mass flow rate due to the higher viscosity of the vegetable fuel.

With reference to fuel conversion efficiency, no significant difference between diesel and WVO was revealed. NO_x emissions were also found as roughly the same. On the contrary, THC and CO emissions were considerably higher for the WVO, but only at low load, probably due to greater mixing difficulties of the WVO, when the turbulences and the temperatures in the combustion chamber get lower.

Journal of Physics: Conference Series **1868** (2021) 012014 doi:10.1088/1742-6596/1868/1/012014

For the DF power supply, the fuel injection laws and the percentage of replacement of the WVO with syngas were varied (30% to 80% by mass). The former was changed by moving both the pilot and the main injections forward or backward with respect to the SOI value stored in the control unit. In figure 1.a, it is possible to see how at 90 Nm both high injection advances and high syngas percentages contribute to a reduction in THC and thus to high combustion efficiencies. The syngas percentage has a non-linear effect on THC emissions, while the advance of the pilot injection always leads to an improvement. As concerns the maximum pressure gradient shown in figure 1.b, an injection advance represents the determining factor, though high percentages of syngas mitigate this increase.
For tests in DF with syngas, the advance of injection of WVO was limited by the reliable operating conditions of the engine, identified by not exceeding the threshold of 15 bar/CAD for the peak of the pressure gradient in the combustion chamber. Feeding with syngas at 80% by mass, compared to the total fuel introduced into the combustion chamber, is equivalent to an energy contribution of about 40%. As the percentage of replacement of WVO with syngas increases, there is a change from combustion with a pre-mixed phase followed by a diffusion phase, to combustion more similar to what occur in a SI engine, with a heat release curve almost symmetrical with respect to the gravity centre. The benefit on THC emissions, both injection advance and of the syngas percentage, is due to a greater completeness of combustion, especially in the areas least affected by the presence of the pilot WVO. This is due to better conditions for the propagation of the flames from the different ignition points due to the pilot. Obviously, as the percentage of replacement with gaseous fuel increases, the concentration of syngas in the flame-extinguishing areas also increases, so the effect on THC is not linear. At the same time, the transition towards a combustion process more similar to that which occurs in a SI engine contributes to reducing the peak of the pressure gradient. This is because the propagation of the flame fronts, triggered by the pilot fuel, makes smoother the heat release curve.

Table 1. Engine performance with full diesel oil and full WVO fuelling.

	Fuel flowrate (kg/h)	Rail pressure (bar)	THC (g/kWh)	CO (g/kWh)	NO_x (g/kWh)	Efficiency (%)
Diesel						
60 Nm	2.7	478	0.3	1.0	3.1	30.3
90 Nm	3.6	624	0.2	0.3	4.6	34.4
120 Nm	4.5	806	0.2	0.3	6.2	35.4
WVO						
60 Nm	2.9	562	0.8	2.4	2.8	31.3
90 Nm	3.8	726	0.3	0.5	4.9	36.0
120 Nm	5.1	953	0.2	0.4	6.8	36.4

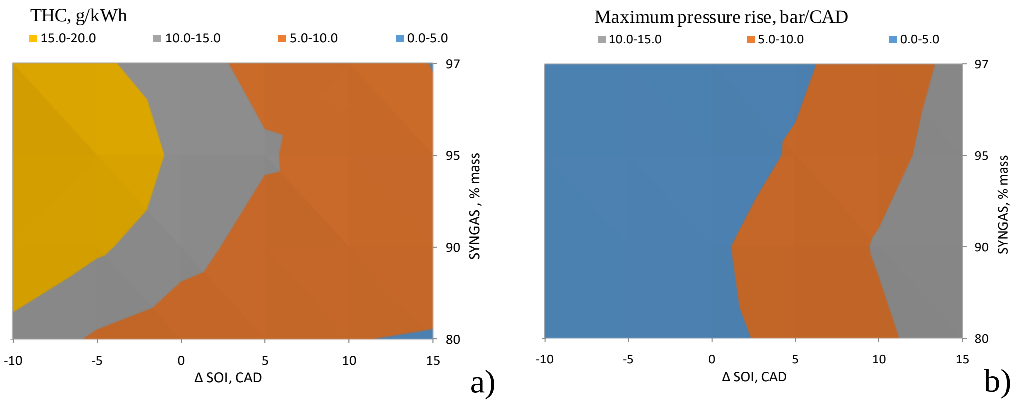

Figure 1: Effect of SOI and variation of syngas mass share on THC emission (a) and maximum pressure rise (b) of DF running at 90 Nm.

3. 3D CFD Model

The three-dimensional (3D) Computational Fluid Dynamics (CFD) model of the considered engine is developed in the AVL Fire™ environment, where the simulated cycle is limited to the closed valve period, from the time of Intake Valve Closing (IVC) to that of Exhaust Valve Opening (EVO). Simulations follow the Reynolds Averaged Navier Stokes (RANS) approach, with the k-ζ-f model is employed for turbulence closure [8]. The balance equations of mass, momentum and energy for the gaseous phase are written in a Eulerian framework, while the liquid spray dynamics is described on a Lagrangian specification through the Discrete Droplet Method (DDM) [4]. Assuming an identical spray evolution for each of the seven injector holes, the combustion chamber is modelled as a 1/7 sector to reduce the associated computational time. The grid is characterized by a first grid boundary node at approximately 1 mm from the wall, where y+ value is around 30–35 to correctly reproduce the log-law profile for turbulent flows. Boundary conditions derive from experimental measurements, while the initialization of turbulent kinetic energy is imposed at the IVC time, according to relations taken from the literature [4]. Due to lack of experimental data, the validation of the Diesel spray dynamics (here not shown) is performed by comparing the simulated penetration length with the one of a single Diesel injection event provided by the considered injector under non-evaporative conditions [9]. The spray parameters tuned for the model validation under Diesel fuelling are then left unchanged when considering WVO, due to lack of experimental data provided in literature for its validation. However, it was demonstrated in a previous publication [10] that the CFD model correctly reproduces the WVO injection characteristics in terms of longer penetration lengths (at fixed SOI and injection pressures), consequence of the higher fuel viscosity, and slower rates of evaporation due to the higher fuel density, with respect to Diesel injection. However, the WVO fuel temperature was increased up to 75° in the CFD model as performed in the experimental tests.

3.1 Combustion under WVO fueling

The combustion process is modelled through the ECFM-3Z model [11], tuned against the experimental pressure cycles by changing the value of the autoignition model parameter responsible for the ignition delay. This last was maintained constant for all the investigated loads to assess the predictive capabilities of the model. For the sake of brevity, only the comparison with WVO fuelling is here shown, made referring to an averaged pressure cycle over 100 consecutive measurements.

Fatty Acid Methyl Esters (FAME) fuels derived by vegetable oils are employed from the AVL Fire™ library. In fact, it has been assessed in a previous publication [10] how the physical and chemical characteristics of these vegetable fuels are close to the ones gathered from the analysis performed on a WVO sample employed in the experimental campaign, allowing to faithfully employ this surrogate fuel for the simulation of the CI engine under WVO fuelling. The agreement is considered satisfactory in both the pressure and Rate Of Heat Release (ROHR) evolutions at different loads, as shown in figure 2. Moreover, the comparison between the masses of produced pollutants is reported in figures 3. NO formation follows the thermal mechanism of Zeldovich [12], while a detailed chemical reaction scheme is employed to evaluate the interaction between the formation and oxidation of soot, the radiative heat loss and the flow-field in turbulent diffusion flames [13]. A satisfying agreement is achieved, well reproducing both the order of magnitude and the trend with load.

3.2 Combustion simulation under dual–fuel operations with WVO and ternary syngas

The employed ECFM-3Z model solves the transport equations of the species representing the molecule representing the injected liquid fuel, O_2, N_2, CO_2, CO, H_2, H_2O, O, H, N, OH. The absence of CH_4 in the combustion model required to substitute the amount of this species with a certain amount of H_2, whose primary power is equivalent with the one characterizing the CH_4 species. The error associated with this approximation can be said limited, as only the operative cases with high load (120 Nm) and low percentages of trapped syngas (30%) are here reproduced. In fact, syngas deriving from biomass gasification is generally characterized by a methane mass fractions below the 2%, as seen in the next section, thus this operation can be considered acceptable with faithful level of confidence also in the case of real syngas combustion [3].

To assess the predictability of the proposed approach, three operative cases at 120 Nm, but different Start Of Injection (SOI), are considered, respectively equal to +10° and -10° with respect to the reference value. It must be pointed out that when retarding the injection phase, a higher amount of trapped syngas in the combustion chamber is required to achieve the same load. The comparison between the pressure and ROHR cycles reported in figure 4 enlighten how, as the SOI is retarded, a numerical underestimation of the start of the diffusive combustion phase occurred. This is a direct consequence of the increased amount of H_2 trapped in the combustion chamber, which also enhances the rate of flame propagation during the premixed phase, as noticed by the pressure spike at the Top Dead Center (TDC) for retarded SOI (figure 4.b). The substitution of methane with H_2 also directly affects the pollutant emissions, as shown in figure 5. The lower amount of carbon in the combustion chamber reduces the amount of CO and CO_2 estimated at the EVO. Moreover, the CO decreasing trend with the SOI is not numerically respected, as the H_2 substituting the trapped methane enhances the combustion efficiency with respect to the experimental tests. As regards the NO estimation, the amount at the EVO is again under-estimated, although the trend is well respected with respect to SOI.

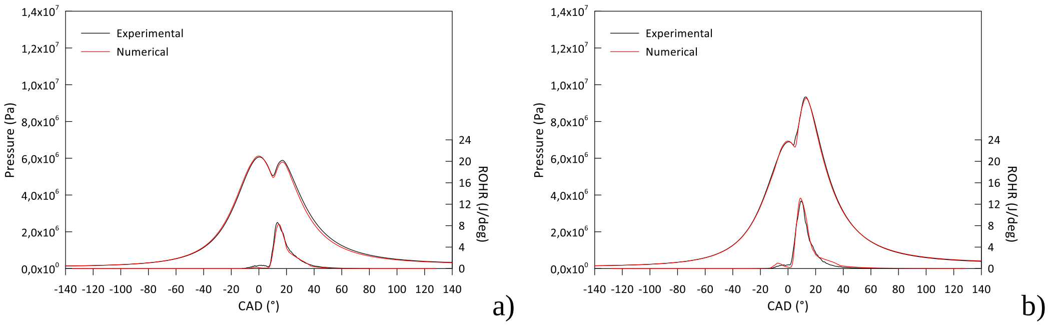

Figure 2: Comparison between the experimental and numerical pressure cycles of the engine under WVO fuelling: a) 60 Nm, b) 120 Nm.

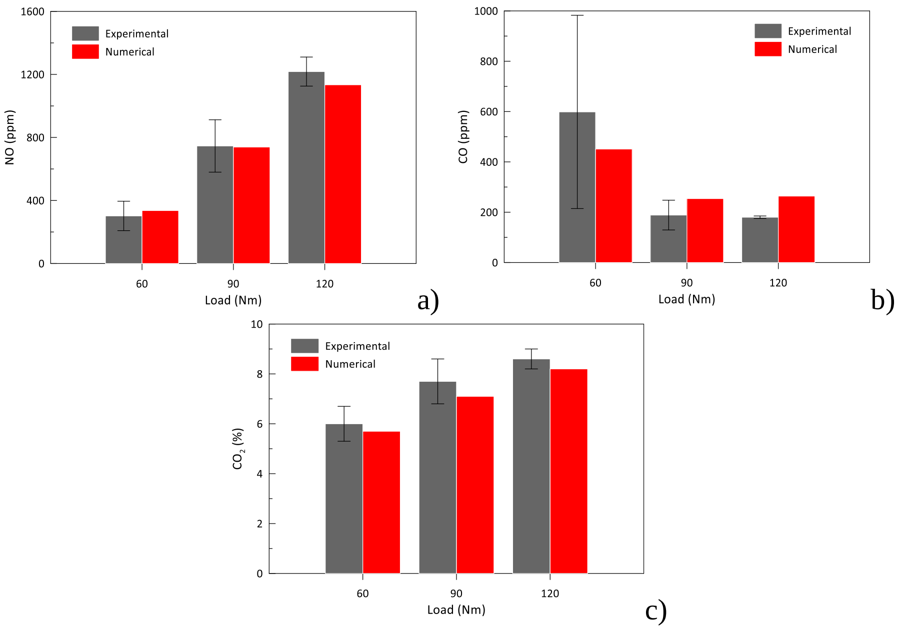

Figure 3. Experimental and numerical comparison between pollutants emissions of the engine under WVO fuelling at different loads: a) NO, b) CO, c) CO_2.

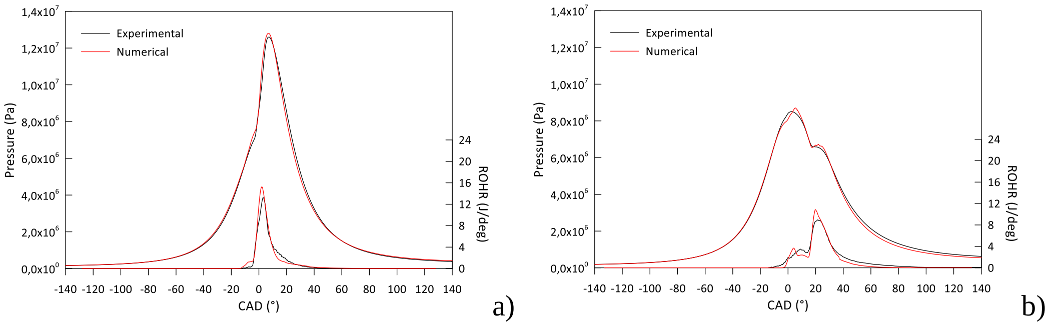

Figure 4: Comparison between the experimental and numerical pressure cycles of the engine under dual–fuel operations at 120 Nm and SOI equal to: a) +10°, b) -10°.

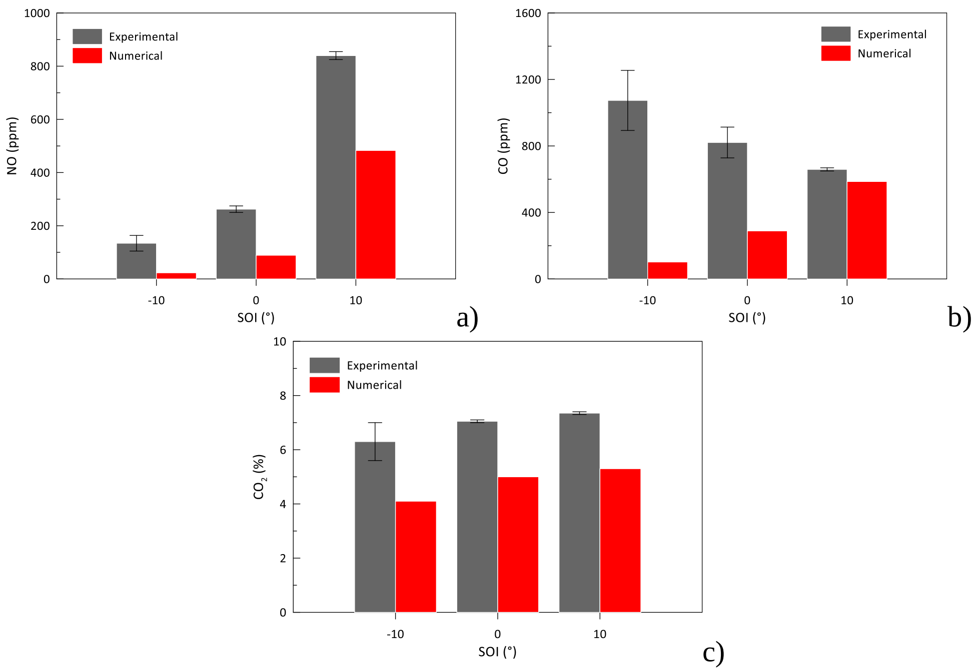

Figure 5. Experimental and numerical comparison of the pollutants emissions of the engine under dual–fuel operations at 120 Nm and different SOI: a) NO_x, b) CO, c) CO_2.

4. CFD simulation of dual–fuel operation with WVO and real syngas

In this section, the performances of the CI engine under dual–fuel operations with real syngas, deriving from gasification of sewage sludge are estimated, by employing the previously validated 3D CFD model. Indeed, despite the numerical underprediction of the noxious emissions deriving by replacing CH_4 with an energetically equivalent amount of H_2, the prediction of the pressure and ROHR cycles is not affected at all loads. Therefore, the comparison of the engine performances under ternary and real syngas fuelling can be performed with faithful confidence.

Syngas composition is estimated through a validated thermodynamic equilibrium model developed by authors [3] at a gasification equivalence ratio of 0.3 and reported in terms of mass fractions in the following table 2, compared with the ternary syngas employed in the experimental tests. Again, table 2, also reports the syngas composition employed in the simulation, after the substitution of the CH_4 with an energetically equivalent H_2 amount. The simulated operative conditions refer to a load of 120 Nm and a SOI equal to 0° with respect to the reference value. A consistent comparison between the engine performance under dual–fuel operation with ternary and real syngas is obtained. For this purpose, the flow rate of the real syngas, characterized by an equivalent primary energy of the ternary syngas, is here evaluated. In the specific, the primary power of the ternary syngas is equal to 23.3 kW and by a flow rate of 15.4 kg/h in the operative condition under study. Therefore, considering the mass fraction of the

CO, H_2 and CH_4 species as in table 2, the flow rate of the real syngas with an equivalent primary power is equal to 15.9 kg/h, thus just the 3.2% higher than the ternary mixture. Therefore, it can be said that the comparison here performed is made by considering two gaseous fuels with the same primary power and similar flow rate. For the sake of clarity, it must be said that if the real syngas is considered, the trapped percentage in the combustion chamber is equal to the 50%, while the ternary mixture under study refers to a 30% percentage. The initial and boundary conditions imposed in the 3D CFD simulation are left unchanged with respect to the operative conditions considered in the previous section. The comparison between the pressure and ROHR cycles shown in the following figure 6 shows similar trends. Indeed, the peaks of premixed and diffusive combustion phases are positioned at the same crank angle, while the indicated power produced under real syngas is just the 4% lower with respect to a ternary mixture. This is an obvious consequence to the presence of inert species in the combustion chamber (H_2O, CO_2) that inhibit the flame propagation and actually reduce the virtual displacement in the combustion chamber. On the other hand, the real syngas has a greater influence on the noxious species, as can be seen in figure 7. Indeed, although the NO produced at EVO is just the 6% lower (because of the lower temperature in the combustion chamber), the CO and CO_2 mass fraction at the EVO are respectively 5.1 and 1.8 times higher.

Table 2: Comparison between the composition of ternary and real syngas coming from gasification of wastewater sewage sludges.

w/w%	Ternary	Real	Simulated
CO	-	2,1	2,1
CO_2	-	3,2	3,3
CH_4	-	0,5	-
H_2	0,6	0,15	0,38
H_2O	-	0,8	0,83
N_2	79,21	73,05	73,39
O_2	20,19	20,2	20

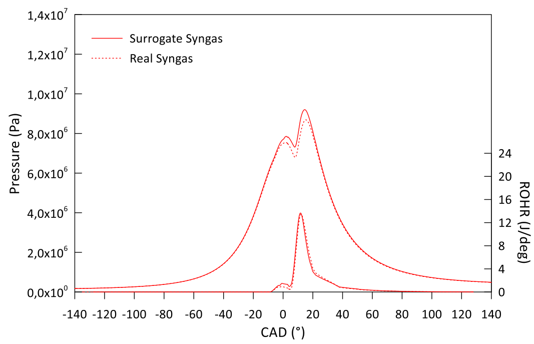

Figure 6. Comparison between the pressure and ROHR evolutions deriving from the 3D CFD simulations in dual–fuel conditions with ternary (red line) and real (red dotted line) mixtures.

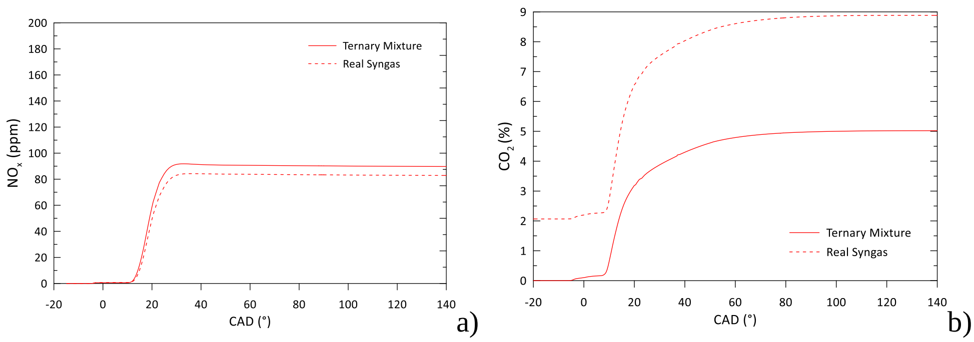

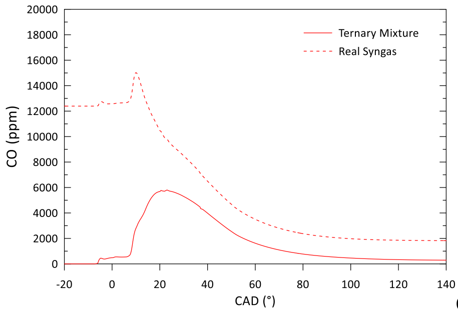

c)

Figure 7. Noxious emissions from 3D CFD simulations up to EVO in dual–fuel operations with ternary and real syngas: a) NO_x, b) CO_2, c) CO.

5. Conclusions

Main results of the performed analysis are the following:

- a 30% WVO mass must be injected in the combustion chamber to achieve the same power obtained under Diesel fuelling, due to the lower calorific value of the renewable fuel;
- high percentages of a ternary mixture of syngas can be trapped in the combustion chamber, assuring reliable performances if the SOI is correctly tuned. Lower NO_x and CO_2 are achieved at the exhaust with respect to the exclusive WVO fuelling;
- employing real syngas from sludge gasification leads to a 4% decrease of power produced with respect to the ternary syngas employed in the experimental tests. On the other hand, influence over the noxious emissions is stronger, as CO and CO_2 respectively increase with a ratio equal to 5.1 and 1.8, respectively.

Aknowledgements

The authors would like to thank Vicenzo Bonanno for his valuable support in experimental activities. The research is a part of the project "PANACEA - Polygeneration from residual biomasses in urban wastewater treatment plants", funded by Ricerca di Sistema Elettrico Nazionale (RdS) of the Italian Ministry of Economic Development.

References

[1] Dewangan A, Mallick A, Yadav AK and Kumar R 2020 Combustion-generated pollutions and strategy for its control in CI engines: A review, *Materials Today: Proceedings* **21** pp. 1728-33.
[2] Costa M and Piazzullo D 2018 Biofuel powering of ICEs: production routes, effect on performance and CFD modeling of combustion *Frontiers in Mechanical Engineering* **4** p. 9.
[3] Costa M, La Villetta M, Massarotti N, Piazzullo D and Rocco V 2017 Numerical analysis of a compression ignition engine powered in the dual-fuel mode with syngas and biodiesel *Energy* **137** pp. 969-79.
[4] Azimov U, Tomita E, Kawahara N and Dol SS 2012 Combustion characteristics of syngas and natural gas in micro-pilot ignited dual-fuel engine *Int. J. Mech. Mechatron. Eng*. **6(12)** pp. 2863-70.
[5] Tarabet L, Loubar K, Lounici MS, Khiari K, Belmrabet T and Tazerout M 2014 Experimental investigation of DI diesel engine operating with eucalyptus biodiesel/natural gas under dual fuel mode, *Fuel* **133** pp. 129-38.
[6] Nayak C, Achrya SK and Swain RK 2016 Performance of a twin cylinder dual-fuel diesel engine using blends of neat Karanja oil and producer gas *Int. J. Amb. Energy* **37(1)** pp. 36-45.
[7] Capuano D, Costa M, Di Fraia S, Massarotti N and Vanoli L 2017 Direct use of waste vegetable oil in internal combustion engines *Renew. Sust. Energy Rev.* **69** pp. 759-70.
[8] Hanjalic K, Popovac M and Hadziabdic M 2004 A robust near-wall elliptic-relaxation eddy-viscosity turbulence model for CFD *Int. J. Heat Fluid Flow* **25** pp. 1047-51.

[9] Mancaruso E, Marialto R, Sequino L, Vaglieco BM and Cardone M 2015 Investigation of the injection process in a research CR diesel engine using different blends of propane-diesel fuel *SAE Technical Paper* 2015-24-2477.
[10] Costa M, Marchitto L, Piazzullo D and Prati MV 2020 Comparison between the energetic and environmental performance of a combined heat and power unit fueled with Diesel and waste vegetable oil: an experimental and numerical study *Submitted to Ren. Energy*.
[11] Colin O and Benkenida A 2003 The 3-zones extended coherent flame model (ECFM-3Z) for computing premixed/diffusion combustion *Oil Gas. Sci. Technol. Rev* **58** pp. 47-62.
[12] Zeldovich YB, Sadovnikov PY and Frank-Kamenetskii DA 1947 Oxidation of nitrogen in combustion *Academy of Sciences of USSR, Institute of Chemical Physics*.
[13] Wang H and Frenklach M. 1997 A detailed kinetic modeling study of aromatics formation in laminar premixed acetylene and ethylene flames *Combust. Flame* **110** pp. 173-221.